FACTA UNIVERSITATIS
Series: **Mechanical Engineering** Vol. 21, Nº 1, 2023, pp. 121 - 135
https://doi.org/10.22190/FUME210507063M

Original scientific paper

ACCURACY ANALYSIS OF THE CURVED PROFILE MEASUREMENT WITH CMM: A CASE STUDY

Tomasz Mazur[1], Miroslaw Rucki[1], Yuriy Gutsalenko[2]

[1]Kazimierz Pulaski University of Technology and Humanities in Radom, Poland
[2]National Technical University "Kharkiv Polytechnic Institute", Kharkiv, Ukraine

Abstract. *In the paper, analysis of the curved profile measurement accuracy is described. Since there was no CAD model or other reference profile for the measured detail, the first step was to generate the reference contour of the cam using the technical drawing and tolerance requirements. The test campaign consisted of three experiments aimed at determining the effect of scanning velocity on the results of form deviation δ measurement, evaluation of deviation δ measurement uncertainty and the measurement repeatability. The scanning time was checked, too. The obtained results demonstrated feasibility of the chosen CMM and measurement strategy. It was found also that the measurement uncertainty did not depend on the scanning sampling step from 0.05 to 0.2 mm, and the true measurement time was for 30-40% longer than that expected from the nominal scanning velocity.*

Key Words: *Curved Profile, Tolerance, Measurement, CMM, Uncertainty*

1. INTRODUCTION

Free-form surfaces and curved profiles are widely used in the design and manufacturing of details with high and strict precision requirements [1,2]. During the machining process, vibrations and other inaccuracies may affect the final state of the curved profile, which leads to the necessity of thorough dimensional and shape inspection to ensure its functionality. Thus, the characterization of free-form surfaces is an increasingly important area of metrology [3]. In particular, tolerance of the profile along with the position tolerance is a crucial feature in the design and manufacture of products with curved profiles.

The contour of curved profiles can be detected either by sensing or by measuring, and measurement systems are generally based on mobile or stationary coordinate measurement systems with specific software and sensors [4]. The accuracy of the results from coordinate

Received May 07, 2021 / Accepted October 20, 2021
Corresponding author: Miroslaw Rucki
Kazimierz Pulaski University of Technology and Humanities in Radom, Malczewskiego 29, 26-600 Radom, Poland
E-mail: m.rucki@uthrad.pl

measurements depends on the accuracy of the measuring device, workpiece properties, environmental conditions, and especially on the operator and measurement procedures [5]. Appropriate planning of a measurement strategy for free-form surfaces is addressed in many publications. For example, it was proposed to establish the local geometric deviation, namely, the difference between each measurement point and the CAD model of the measured surface [6]. Other papers dealt with two key problems of surfaces and curves profile error measurement: (1) evaluation algorithm of profile error on the basis of minimum zone principle or maximum material condition; (2) computer aided arbitrament for minimum zone principle and maximum material condition [7]. For the measurement of freeform shaped workpieces, the distortions caused by the tip mechanical filtration have impact on measurement accuracy, so that correction is desired in order to restore to the real workpiece surface [8]. Menq and Chen noted that after measurement with a contact probe, the generated surface differed from the real one because of the radius compensation errors of the probe. Minimization of the compensation errors required that the probing directions of the CMM coincide with the normal vectors of the probed points. They emphasized unavailability of the normal vectors of data points when the CAD model of a new design did not exist [9]. Similarly, in 3D gear measurements, the influence of CMM geometric errors on the results is still unclear because the requirement for a gear measurement standard with ideal geometry cannot be fulfilled [10]. It should be noted that the laser-based measurement methods of curved profiles need compensation, too [11].

A significant share in the overall calculus of errors in scanning measurements performed on coordinate measuring machines (CMM) refers to dynamic errors [12]. Since the measurement time and cost increase proportionally as the increase of sampling points, it is essential to study a sampling method [13].

The volumetric probing uncertainty of a CMM is usually determined adding a component of the length measuring uncertainty, considering the distance between 25 points on the calibrating sphere, to get the overall point coordinate uncertainty of the CMM [14]. Evaluation of repeatability and reproducibility of the CMM equipment is necessary, too [15]. Prior to numerical characterization, filtering is done and it is also essential for extracting information needed to provide process feedback and establish functional correlation [16]. A study of roundness of different artifacts using different algorithm and filters demonstrated impact of filtering on the measurement results [17]. The number of CMM points in the measurement of each feature of a part has to enable achievement of a simulated feature-fit that results in a high-quality representation of the manufactured feature [18]. In order to simplify the calculation and simultaneously retain the accuracy of evaluation, the method was proposed, based on the extraction of key points from scanning data set [19]. Other authors emphasized, however, that the simulation of measurement became very complicated when the solution of the measuring task needed construction of elements using measured features [20]. Some authors emphasized that there are very few commercially available software systems that offer sweep scan path planning function. Moreover, newly proposed methods able to generate a viable sweep scan path automatically require significant user's knowledge and involvement [21].

From that perspective, it is crucial to keep consistency in the measurement procedure. A dictionary definition of 'consistency' is 'constant adherence to the same principles of thought or action' [22]. Saunders and co-authors noted that this definition is intended to refer to a personal characteristic, but since many personal choices are made during programming,

operating, and evaluating of the CMM measured points, the term also works well within the context of measurement [23].

According to the definition of the profile tolerance in ISO 1101 [24], the surface profile error can be defined by the minimum diameter covering all measured points of the cluster spheres whose centers lie on the design model. Profile tolerance may be related to a basic surface; then its orientation and position are dependent on the definition of bases and base-dependent coordinate system.

Researchers have proposed various practical approaches towards evaluating form deviations of 2D contour profiles based on coordinate measurement data. For example, a 2D contour was divided into straight and curved parts [25]. There are reports in which extracted points of curved profile deviated from reference data within ±0.1 mm [26]. In the present paper, we focused on the statistical analysis of the results obtained for the curved 2D profile with no available CAD model. The measurement results appeared to be dependent on the scanning parameters, so that a balance between accuracy demands and measurement time had to be found. Also the problem of basic surface for measurements was challenged in order to keep consistence of the results.

2. Materials and Methods

In the research studies, a cam with complex 2D profile curvature was measured. Its dimensions and tolerances are shown in Fig. 1. Its form tolerance was 0.15 mm , and roughness of curved surface was limited to Ra = 1.25 µm and Rz = 6.3 µm. Using the data from Fig. 1, theoretical (reference) profile was generated as a file *.dxf using the program SolidWorks 2019.

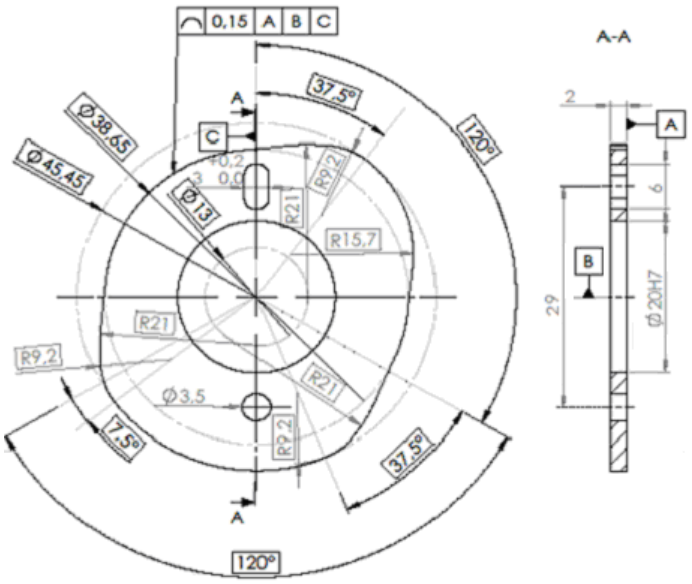

Fig. 1 Technical drawing of the measured cam

The contour of the cam was generated using the technical drawing, and in form of *.dxf file was input to the CMM control program. In the file, 2829 theoretical (reference) points constituted the profile with coordinates x, y, z in the local coordinate system (LCS) defined according to the technical drawing. The points were located approximately uniformly 1 mm below the base surface of the cam, i.e. z = -1 mm for each point. The length of the contour was l_c = 123,49 mm.

The measurements were performed with the CMM Mitutoyo Crysta – Apex S 7106. It is a high-accuracy CNC coordinate measuring machine that guarantees a maximum permissible error defined by ISO 10360-2:2009 of $E_{0,MPE}$ = (1.7+3L/1000) μm at ambient temperature 20 ±2 °C. L stands for the selected measuring length in mm. The measuring range in three axis is x = 700; y = 1000; z = 600 mm, 3D acceleration a = 2309 mm/s^2, and linear velocity in three directions x, y, z is v = 519 mm/s.

Moreover, the CMM has temperature compensation function in the range of 16÷26 °C, which makes it suitable for working in the industrial conditions. The machine can be equipped with contact scanning probe, non-contact laser probe or vision probe [27]. Scanning mode makes it possible to perform measurement with 0.05-1.0 point-point step or distance between points, scanning speeds between 0.5 and 4 mm/s, and permissible probe deflection in the range from 0.15 to 0.4 mm.

Fixation of the cam with defined LCS is shown in Fig 2. Fig. 3 presents the initial window of CMM for scanning of an outer closed contour with the set values described below in the text.

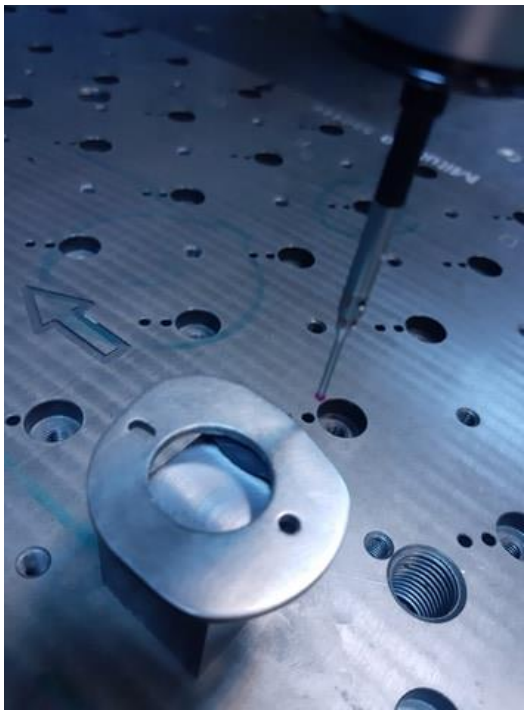

Fig. 2 Fixation of the measured cam on the CMM table

To perform the experiments, control software MCosmos was used. In this program, ready scripts are available for the measurement of all standardized geometrical tolerances, as well as the measurement of complex shapes in local coordinates.

Before the measurement, a fixture was made so that the entire profile could be measured in one fixation with one probe. The probe was calibrated with the calibration sphere, and a local coordinate system (LCS) was defined according to the tolerance data provided in the drawing Fig 2. The LCS definition covered following elements:

- base A as a head surface of the measured cam became the main surface of the LCS, it defined axes *X* and *Y* from 4 measuring points,
- base B defined LCS center in the center of the hole Ø20, using 4 points of the circle,
- base C as a line connecting three points, two of them lay in the bisector of the first smaller base hole and the third one was the center of the second smaller base hole; it was moved in parallel up to base B become axis Y,
- remaining axes *x* and *y* are derived from the right-hand coordinate system.

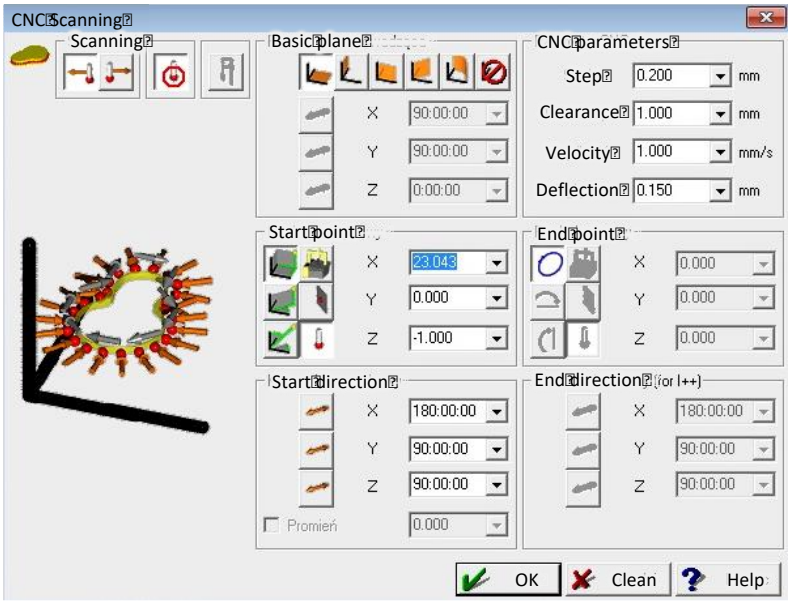

Fig. 3 Window of the MCosmos program for the measurement parameters

During the measurement, the CMM program written for that specific purpose is collecting the coordinates of measuring points. According to the definition of the profile deviations, it registers maximal deviation value $\delta_{max}$and shows its position in the profile. The number of collected points is dependent on the measurement step and only approximately corresponds to the profile length divided by step. Apart from deviation value δ, scanning time was registered directly by the CMM program.

After the measurement is finished, the program records automatically the measurement report with the value of the largest registered deviation from the reference profile. Moreover, the program makes it possible to register all the measuring points from the scanning, in the respective file *.dxf.

3. TEST CAMPAIGN

The test campaign consisted of three experiments aimed at determining the effect of scanning velocity on the results of form deviation δ measurement, evaluation of deviation δ measurement uncertainty and the measurement repeatability.

During the profile scanning, three parameters could be set:

- scanning velocity v_s in the range between 0.5 and 4 mm/s,
- permissible probe deflection p_d in the range between 0.15 and 0.4 mm, and,
- scanning step s between 0.05 and 1 mm.

The respective values used in each measurement series are presented in the Table 1.

Table 1 Parameters of experimental measurements

Series No.	v_s [mm/s]	p_d [mm]	s [mm]	Number of repetitions n
1	1	0.15	0.2	5
2	1	0.2	0.2	5
3	1	0.3	0.2	5
4	1	0.4	0.2	5
5	2	0.15	0.2	5
6	2	0.2	0.2	5
7	2	0.3	0.2	5
8	2	0.4	0.2	5
9	3	0.15	0.2	50 (3×5+1×10+1×25)
10	3	0.2	0.2	5
11	3	0.3	0.2	5
12	3	0.4	0.2	5
13	4	0.15	0.2	5
14	4	0.2	0.2	5
15	4	0.3	0.2	5
16	4	0.4	0.2	5
17	3	0.15	0.2	50
18	3	0.15	0.05	50

The above-mentioned parameters were chosen in order to perform three different experiments, as explained below.

3.1. Effect of scanning velocity on results of the form deviation measurements

In the first set of experiments, the goal was to determine the effect of different scanning velocities v_s on the results of profile form deviation, considering the measurement time. In this set of measurements, the scanning step remained unchanged, s = 0.2 mm. As shown in the Table 1 above, the measurements were performed for 16 combinations of v_s and p_d settings. For each combination, the measurements were repeated 5 times. The number of measuring points differed in a small range from 645 up to 660.

3.2. Uncertainty evaluation

It can be assumed that the factors having effect on the measurement uncertainty of a cam contour are similar to the ones typical for roundness measurement [28-29]. Uncertainty analysis was performed using the Type A approach [30] with 50 repetitions made in the

repeatability conditions. Two series of measurements marked 17 and 18 in Table 1 had similar parameters v_s = 3 mm/s and p_d = 0.15 mm, but different sampling step. This experiment was to demonstrate how the uncertainty of form deviation is dependent on the number of probing points. In the series 17, at sampling step s = 0.2 mm, the number of probing points was ca. 650, while in the series 18 it was 2560-2590, close to the respective number in the reference file *.dxf.

3.3. Repeatability in short measurement series

Considering a relatively long time of a single measurement, which can be as long as 200 s at scanning speed v_s = 1 mm/s, it is reasonable to expect that 50 repetitions may not completely conform to the repeatability conditions requirement. To challenge this issue, the third experiment was performed. In the case of the series 9 (Table 1, v_s = 3 mm/s, p_d = 0.15 mm, s = 0.2 mm), the measurement was firstly performed three times with 5 repetitions each time, then with 10 repetitions, and finally with 25 repetitions. This procedure was described in Tab. 1 as 3×5+1×10+1×25. Thus, the strict repeatability conditions were kept only for each group of repetitions, but not only for the entire sample of 50 similar measurements. As a result, measurement repeatability for a smaller number of repetitions could be compared with the results for a larger number.

All these measurements, as well as the ones described in Section 3.1, were performed on the same day, with no resetting the CMM. After calibration of the probe, the measured cam was not moved from its fixed position. The coordinate system once established was applied to each measurement due to the specially prepared software program. Moreover, to assure a higher level of repeatability, the initial position of the probe before each measurement was identical.

The experiments described in Section 3.2, however, were performed several months later, and for each of them the CMM was started anew. In this way the obtained results in series 17 and 18 must be treated as two separate experiments, while the others are somewhat interconnected between each other through the same definition of the coordinate system and a relatively short time between the repetitions.

4. Results and Discussion

Overall number of the maximal deviation measurement results was 225. In order to determine normality of the results distribution, the Kolmogorov-Smirnov test was applied to each of tests with 50 repetitions, namely, series No. 9, 17 and 18, as described in the previous section. Respective D-values of the statistics were 0.1789, 0.14551 and 0.18754, while p-values were 0.07, 0.22 and 0.05, respectively. Hence the measurement results in the series did not differ significantly from Gaussian distribution, despite some differences in statistical parameters. Fig. 4 presents the respective histograms.

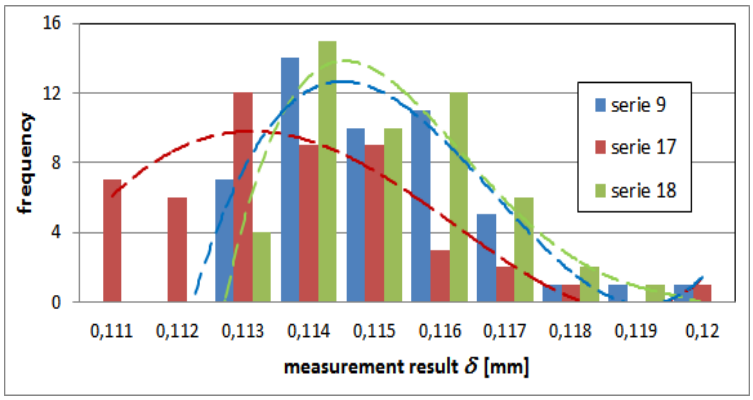

Fig. 4 Histograms of the measurement results of 50 repetitions in the series No. 9, 17, and 18

Knowing that the distribution of form deviation δ measurement results is normal, it is possible to apply the Student-Fisher parameters to the smaller series of 5, 10 and 25 repetitions. Thus, confidence interval CI can be calculated as follows:

$$CI = t_{\alpha,n-1} \times S_n \tag{1}$$

where: $t_{\alpha,n-1}$ – Student-Fisher distribution quantile, n – number of the repetitions in series, S_n – standard deviation.

Assuming confidence level $P = 0.99$, the respective quantile value for 5 repetitions is $t_{\alpha,n-1} = 4.604$, for 10 repetitions $t_{\alpha,n-1} = 3.250$, and for 25 repetitions $t_{\alpha,n-1} = 2.797$ [31].

4.1. Effect of scanning velocity on form deviation

In Tables 2-5, there are collected measurement results for form deviation δ obtained at different scanning velocities v_s and probe deflection p_d, together with the time of measurement t. The series numbers correspond with the ones specified above in Table 1. Table 4 contains results for probe deflection $p_d = 0.15$ mm only for one series with 5 repetitions.

Table 2 Form deviation δ obtained at $v_s = 1$ mm/s (series 1-4)

	p_d= 0.15 mm		p_d= 0.2 mm		p_d= 0.3 mm		p_d= 0.4 mm	
Repetition No.	δ [mm]	t [s]	δ [mm]	t [s]	δ [mm]	t [s]	δ[mm]	t [s]
1	0.118	198	0.115	179	0.114	156	0.112	145
2	0.120	203	0.116	181	0.113	155	0.112	145
3	0.116	205	0.115	177	0.112	154	0.111	146
4	0.118	201	0.116	177	0.113	155	0.111	147
5	0.119	199	0.118	178	0.115	154	0.112	146
Mean value	0.118	201.2	0.116	178.4	0.113	154.8	0.112	145.8
Standard deviation S_n	0.001	2.864	0.001	1.673	0.001	0.837	0.001	0.837
Confidence interval	0.007	13.18	0.006	7.7	0.005	3.85	0.003	3.85

Table 3 Form deviation δ obtained at v_s = 2 mm/s (series 5-8)

	p_d= 0.15 mm		p_d= 0.2 mm		p_d= 0.3 mm		p_d= 0.4 mm	
Repetition No.	δ [mm]	t [s]	δ [mm]	t [s]	δ [mm]	t [s]	δ[mm]	t [s]
1	0.119	95	0.115	84	0.114	75	0.112	75
2	0.116	97	0.115	84	0.116	77	0.112	75
3	0.115	95	0.115	84	0.112	77	0.114	73
4	0.116	97	0.115	84	0.113	77	0.112	74
5	0.118	95	0.114	84	0.118	78	0.114	74
Mean value	0.117	95.8	0.115	84.0	0.115	76.8	0.113	74.2
Standard deviation S_n	0.002	1.095	0.000	0.000	0.002	1.095	0.001	0.837
Confidence interval	0.008	5.04	0.002	0.000	0.011	5.04	0.005	3.85

Table 4 Form deviation δ obtained at v_s = 3 mm/s (series 9-12)

	p_d= 0.15 mm		p_d= 0.2 mm		p_d= 0.3 mm		p_d= 0.4 mm	
Repetition No.	δ [mm]	t [s]	δ [mm]	t [s]	δ [mm]	t [s]	δ[mm]	t [s]
1	0.120	61	0.117	56	0.116	47	0.113	47
2	0.117	62	0.116	56	0.116	50	0.110	47
3	0.117	63	0.113	57	0.113	50	0.119	49
4	0.116	62	0.115	57	0.115	51	0.114	50
5	0.116	61	0.113	55	0.116	50	0.112	49
Mean value	0.117	61.8	0.115	56.2	0.115	49.6	0.114	48.4
Standard deviation S_n	0.002	0.837	0.002	0.837	0.001	1.517	0.003	1.342
Confidence interval	0.008	3.85	0.008	3.85	0.006	6.98	0.015	6.18

Table 5 Form deviation δ obtained at v_s = 1 mm/s (series 1-4)

	p_d= 0.15 mm		p_d= 0.2 mm		p_d= 0.3 mm		p_d= 0.4 mm	
Repetition No.	δ [mm]	t [s]	δ [mm]	t [s]	δ [mm]	t [s]	δ[mm]	t [s]
1	0.120	50	0.113	46	0.115	42	0.121	38
2	0.118	49	0.115	46	0.117	40	0.114	38
3	0.117	49	0.117	46	0.115	41	0.114	37
4	0.115	47	0.117	46	0.117	41	0.113	37
5	0.117	48	0.117	46	0.111	41	0.118	38
Mean value	0.117	48.6	0.116	46.0	0.115	41.0	0.116	37.6
Standard deviation S_n	0.002	1.140	0.002	0.000	0.002	0.707	0.003	0.548
Confidence interval	0.008	5.25	0.008	0.000	0.011	3.26	0.016	2.52

From the above results, it can be seen that larger permissible probe deflection p_d enabled 22-28% shortening of the measurement time at each scanning speed. However, it caused distinguishable 1-6% reduction of the obtained result of form error δ. Graph in Fig.5 shows how this reduction differs for different scanning speed values v_s.

From Fig. 5 it can be concluded, that at higher scanning speeds, the influence of probe deflection is smaller. For $p_d \leq$ 0.2 mm, speed-dependent differences in obtained form deviations δ lay below $E_{0,MPE}$ = (1.7+3L/1000) μm for the used CMM. Notably, this range of the deflection values ensured insignificant effect of scanning speed v_s on the form deviation results. For each p_d = 0.15 and 0.2 mm, differences between obtained δ at various v_s were 1 μm. Larger probe deflections led to widening of the results span, which indicated

increased uncertainty of the measurement. Due to this observation, we are against application of p_d> 0.2 mm for this sort of measurement.

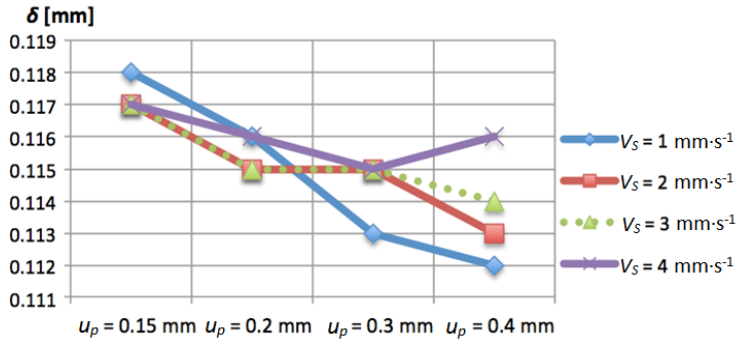

Fig. 5 Form deviation δ obtained at different scanning speeds v_s and different probe deflections p_d

Calculations of true scanning velocity v_s' revealed substantial differences between them and set values v_s. Values of v_s' were determined from the known length of measured contour l_c and automatically registered time of each measurement. Table 6 presents the values and percentage differences between them.

Table 6 True values of scanning speed v_s' related to the nominal ones v_s for different probe deflections p_d (sampling step was 0.2 mm)

	p_d= 0.15 mm		p_d= 0.2 mm		p_d= 0.3 mm		p_d= 0.4 mm	
v_s [mm/s]	v_s' [mm/s]	Percen-tage	v_s' [mm/s]	Percen-tage	v_s' [mm/s]	Percen-tage	v_s' [mm/s]	Percen-tage
1	0.120	50	0.113	46	0.115	42	0.121	38
2	0.118	49	0.115	46	0.117	40	0.114	38
3	0.117	49	0.117	46	0.115	41	0.114	37
4	0.008	5.25	0.008	0.000	0.011	3.26	0.016	2.52

It should be noted that the true scanning speed never reached its nominal value, and smaller probe deflections reduced its value by almost 40%. Considering previous conclusion that the measurement should not be performed with p_d> 0.2 mm, this finding becomes extremely important. In the case of 100% inspection of large lots of the cams similar to the one investigated, measurements will take 30-40% longer time than it would be expected from the nominal scanning speed. In the Flexible Manufacturing Systems working in the frames of Industry 4.0 concept [32], prolonged inspection time may become an issue.

4.2. Results of uncertainty evaluation

In the Type A uncertainty evaluation, three series of the measurement results were used, 50 repetitions each. It can be assumed that the standard uncertainty is approximately equal to the standard deviation $u(x) \approx S_n$, and the coverage factor for the level of confidence p = 99% can be k_p = 2.576 [28]. As described above, series No. 9 followed repeatability

conditions, but not as strictly as series No. 17. On the other hand, series No. 18 had a larger number of probing points, close to that of the reference file derived from the technical drawing. Table 7 presents values of the calculated standard and expanded uncertainties. Examples of the measured profiles with emphasized δ_{max} are shown in Figs 6 and 7.

Table 7 Uncertainty estimation based on the series with 50 repetitions

Series No.	9	17	18
$\overline{\delta}$ [mm]	0.1151	0.1137	0.1152
$S_n \approx u(x)$	0.00158	0.00195	0.00142
$U_{0.99} = k_p \times u(x)$	0.004	0.005	0.004

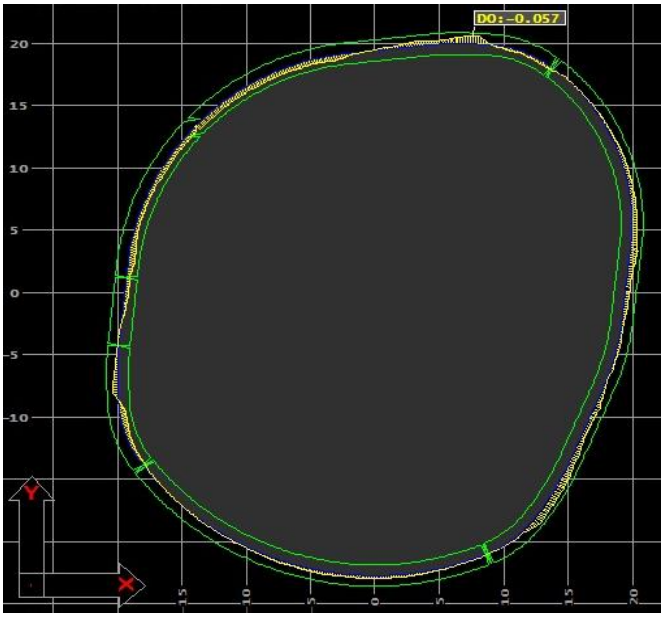

Fig. 6 Example of the measured profile with the result of δ = 0.113 mm; sampling step s = 0.2 mm, 660 probing points

The results presented in Table 7 appear a little unexpected. A higher degree of conformity is between series No. 9 and 18 than between No. 17 and any of two others, despite its conditions were "in-between" (same number of probing points as No. 9 and time of experiment closer to No. 18). Nevertheless, it should be kept in mind that the differences between both mean values $\overline{\delta}$ and expanded uncertainties $U_{0.99}$ for three series lay below $E_{0,MPE}$. Hence, it may be stated that the influence of sampling is negligibly small when estimating the measurement uncertainty of CMM measurement of the cam profile.

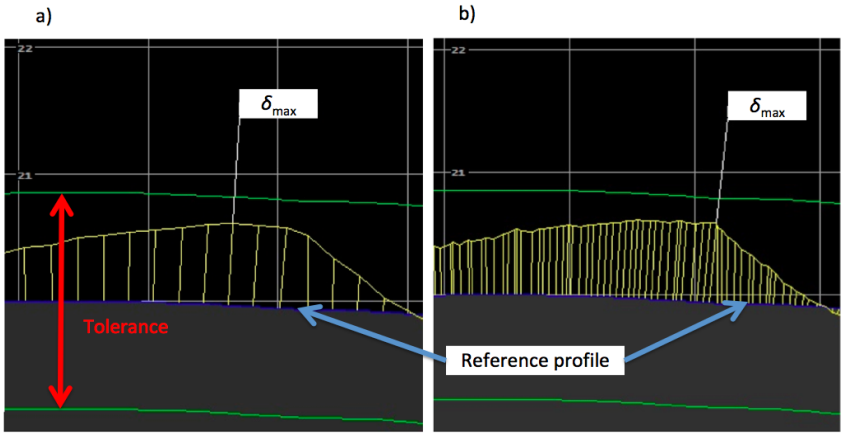

Fig. 7 View of the area with the largest identified form deviation: a) δ_{max} = 0.113 mm after scanning with step s = 0.2 mm, b) δ_{max} = 0.116 mm after scanning with step s = 0.05 mm

This conclusion is confirmed by a detailed analysis of the maximal deviation localization on the cam profile. Irrespective of what sampling step, scanning velocity or probe deflection was applied ,δ_{max} was identified in the same area.

Moreover, it should be noted that a large number of probing points effects in increase of the processing time and, hence, the measurement lasts longer. Experimental evaluation of the uncertainty demonstrated that it is unnecessary, and the results with similar uncertainty may be obtained at a larger sampling step in a shorter time.

4.3. Repeatability in short measurement series

Table 8 presents the results obtained subsequently for the series No. 9, as described in Section 3.3. The first column presents the number of each measurement in the series 9, while the second one is the number of a group, as follows: 5 repetitions in the 1st group, 5 in the 2nd and 3rd, respectively, 10 repetitions in the 4th group and 25 repetitions in the 5th group. For each group, respective standard deviations S_n and confidence intervals CI were calculated both for measured deviation δ and for measurement time t. In the last row, overall statistics is added for the entire series No. 9 for $t_{0.01,49}$=2.6802. Fig. 8 shows the histograms of the results with approximated distribution curves for the group No. 5 and for overall statistics.

Table 8 Statistics for form deviation δ and scanning time t obtained at v_s = 3 mm/s with sampling step s = 0.2 mm and p_d= 0.15 mm in short measurement groups

Group No.	$\bar{\delta}$ [mm]	S_n	CI	$\bar{t}$ [s]	S_n	CI
1	0.1172	0.00164	0.0076	61.8	0.837	3.85
2	0.1150	0.00255	0.0117	65.2	0.447	2.06
3	0.1150	0.00173	0.0080	62.6	0.548	2.52
4	0.1153	0.00125	0.0041	60.4	1.35	4.39
5	0.1146	0.00115	0.0032	62.2	1.165	3.26
Overall	0.1151	0.00158	0.0042	62.2	1.646	4.41

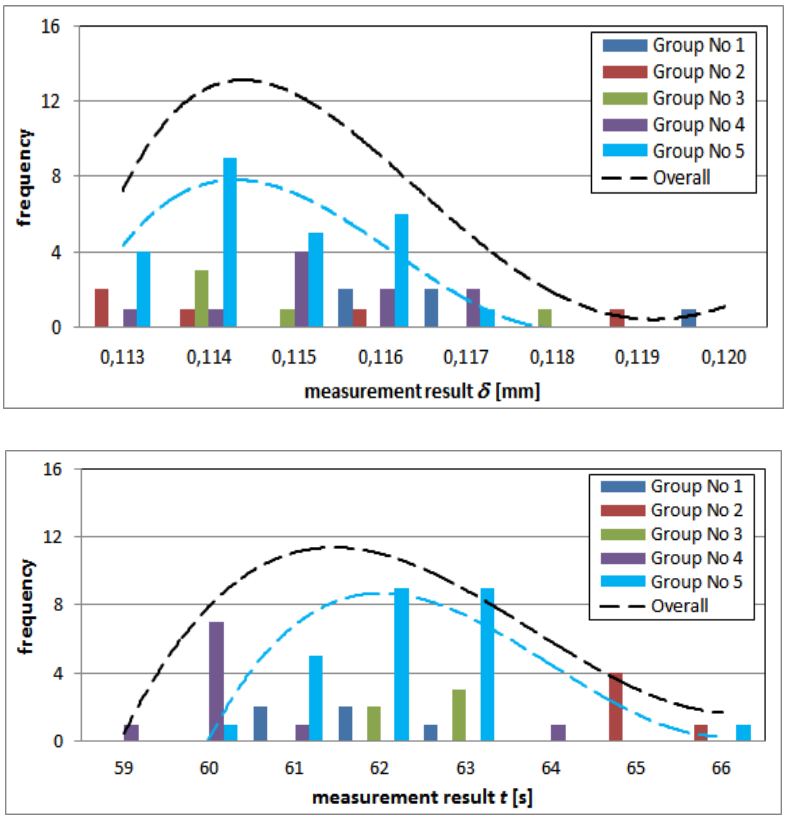

Fig. 8 Distribution of the results in short measurement series: a) deviation δ and b) measurement time t

Interestingly, the first three groups that would be expected to be similar, revealed the following statistics: mean values $\overline{\delta}$ were similar for groups 2 and 3, with 2.2 µm higher $\overline{\delta}$ for group 1, but the respective confidence intervals were similar for groups 1 and 3, with *CI* for the group 2 almost 50% wider. For the groups with 10 and 25 repetitions, confidence intervals reduced substantially, down to 0.0041 and 0.0032, respectively. Notably, mean value $\overline{\delta}$ for group 4 was slightly higher than that for groups 2 and 3, while for group 5 it was slightly lower. The difference was smaller than 0.4 µm, significantly below the maximum permissible error $E_{0,MPE}$ = (1.7+3*L*/1000) µm for the CMM used in experiments.

5. Conclusions

The results of the experimental research studies demonstrated that increased probe deflections p_d reduced the values of measured form deviation. Additionally, p_d higher than 0.2 mm increased the results dispersion. It was found also that the measurement uncertainty did not depend on the scanning sampling step from 0.05 to 0.2 mm, but it should be noted that a smaller step increased the measurement time.

Noteworthy, the true measurement time was for 30-40% longer than that declared by nominal scanning velocity. These characteristics must be taken into consideration when projecting the batch inspection procedures, especially when 100% of parts must be measured. Moreover, there is no necessity in the increased number of repetitions since even a small number of repetitions gave similar mean results with differences close to the maximum permissible error of the CMM.

The most important conclusion is that the highest value of form deviation was identified in the same location irrespective of the applied measurement parameters. Expanded uncertainty of form deviation measurement at the level of confidence $p = 99\%$ was $U_{0.99} = 0.005$ mm, less than 10% of the measured tolerance. This value proved that the chosen CMM as well as the inspection methodology were appropriate for the measurement of the given curved profile.

Acknowledgements: *The paper is a part of the research program conducted at the Faculty of Mechanical Engineering, Kazimierz Pulaski University of Technology and Humanities in Radom, Poland. No specific funds were applied.*

REFERENCES

1. Bo, P., Bartoň, M., 2019, *On initialization of milling paths for 5-axis flank CNC machining of free-form surfaces with general milling tools*, Computer Aided Geometric Design, 71, pp 30-42.
2. Vosniakos, G., Pipinis, G., Kostazos, P., 2021, *Numerical simulation of single point incremental forming for asymmetric parts*, Facta Universitatis-Series Mechanical Engineering, doi: 10.22190/FUME201210046V.
3. Jiang, X. J., Scott, P. J., 2020, *Chapter 10 - Characterization of free-form surfaces*, in: X.J. Jiang, P.J. Scott (Eds.), *Advanced Metrology*, Academic Press, pp. 247-280.
4. Fleischer, J., Munzinger, C., Lanza, G., Ruch, D., 2009, *Position and contour detection of spatially curved profiles on the basis of a component-specific scale*, CIRP Annals – Manufacturing Technology, 58(1), pp. 481-484.
5. Weckenmann, A., Knauer, M., 1998, *The influence of measurement strategy on the uncertainty of CMM-measurements*, Annals of the ClRP, 47(7), pp. 451-454.
6. Poniatowska, M., 2012, *Deviation model based method of planning accuracy inspection of free-form surfaces using CMMs*, Measurement, 45(5), pp 927-937.
7. Xiong, Y.L., 1990, *Computer aided measurement of profile error of complex surfaces and curves: Theory and algorithm*, International Journal of Machine Tools and Manufacture, 30(3), pp. 339-357.
8. Lou, S., Brown, S.B., Sun, W., Zeng, W., Jiang, X., Scott, P.J., 2019, *An investigation of the mechanical filtering effect of tactile CMM in the measurement of additively manufactured parts*, Measurement, 144, pp. 173-182.
9. Menq, C., Chen, F.L., 1996, *Curve And Surface Approximation From CMM Measurement Data*, Computers ind. Engng, 30(2), pp. 211-225.
10. Lin, H., Keller, F., Stein, M., 2020, *Influence and compensation of CMM geometric errors on 3D gear measurements*, Measurement, 151, Article 107110.
11. Ding, D., Zhao, Z., Zhang, X., Fu, Y., Xu, J., 2020, *Evaluation and compensation of laser-based on-machine measurement for inclined and curved profiles*, Measurement, 151, Article 107236.
12. Adam Wozniak, A., Krajewski, G., Byszewski, M., 2019, *A new method for examining the dynamic performance of coordinate measuring machines*, Measurement, 134, pp. 814-819.
13. Zhang Y., Chen, Z., Zhu, Z., Wang, X., 2020, *A sampling method for blade measurement based on statistical analysis of profile deviations*, Measurement, 163, Article 107949.
14. Dhanish, P.B., Mathew, J., 2006, *Effect of CMM point coordinate uncertainty on uncertainties in determination of circular features*, Measurement, 39(6), pp. 522-531.
15. Kubátová, D., Melichar, M., Kutlwašer, J., 2017, *Evaluation of Repeatability and reproducibility of CMM equipment*, Procedia Manufacturing, 13, pp. 558-564.
16. Raja, J., Muralikrishnan, B., Fu, S., 2002, *Recent advances in separation of roughness, waviness and form*, Precision Engineering, 26(2), pp. 222-235.
17. Raghu, S., Mamatha, T.G., Pali, H.S., Sharma, R., Vimal, J.R., Kumar V., 2020, *A comparative study of circularity of artefact detecting circle using CMM and form tester with different filters*, Materials Today: Proceedings, 25(4), pp. 821-826.

18. Kalish, N. J., Davidson, J. K., Shah, J.J., 2020, *Constructive statistics and virtual capture zones: A novel math model for CMM metrology*, Procedia CIRP, 92, pp. 39-44.
19. He, G., Sang, Y., Wang, H., Sun, G., 2019, *A profile error evaluation method for freeform surface measured by sweep scanning on CMM*, Precision Engineering, 56, pp. 280-292.
20. Gąska, A., Harmatys, W., Gąska, P., Gruza, M., Gromczak, K., Ostrowska, K., 2017, *Virtual CMM-based model for uncertainty estimation of coordinate measurements performed in industrial conditions*, Measurement, 98, pp. 361-371.
21. Zhou, Z., Zhang, Y., Tang, K., 2016, *Sweep scan path planning for efficient freeform surface inspection on five-axis CMM*, Computer-Aided Design, 77, pp. 1-17.
22. Oxford English Dictionary. Oxford University Press. (2013) consistency, n. OED Online. Retrieved December 17, 2013, from http://www.oed.com
23. Saunders, P., Wilson, A., Orchard, N., Tatman, N., Maropoulos, P., 2014, *An Exploration into Measurement Consistency on Coordinate Measuring Machines*, Procedia CIRP, Volume 25, pp. 19-26.
24. EN ISO 1101:2017: *Geometrical product specifications (GPS)*.
25. Qiu, H., Li, Y., Cheng, K., Li, Y., 2000, *A practical evaluation approach towards form deviation for two-dimensional contours based on coordinate measurement data*, International Journal of Machine Tools & Manufacture, 40, pp. 259–275.
26. Fan, J., Ma, L., Sun, A., Zou, Zh., 2020, *An approach for extracting curve profiles based on scanned point cloud*, Measurement, 149, Article 107023.
27. CRYSTA-APEX S SERIES, Bulletin No. 2173, Mitutoyo, https://www.mitutoyo.com/wp-content/uploads/2013/01/2097_CRYSTA_ApexS.pdf (Accessed on December, 7, 2020).
28. Gapinski, B., Grzelka, M., Rucki, M., 2006, *The roundness deviation measurement with coordinate measuring machines*, Engineering Review, 26(1-2), pp. 1-6.
29. Gapinski, B., Rucki, M., 2008, *The roundness deviation measurement with CMM*, 2008 IEEE International Workshop on Advanced Methods for Uncertainty Estimation in Measurement, pp. 108-111, doi: 10.1109/AMUEM.2008.4589944
30. JCGM 100:2008. *Evaluation of measurement data — Guide to the expression of uncertainty in measurement*.
31. Jezierski, J., Kowalik, M., Siemiątkowski, Z., Warowny, R., 2010, *Tolerance analysis in the mechanical engineering*, WNT, Warszawa (in Polish).
32. Messinis, S., Vosniakos, G.C., 2020, *An agent-based flexible manufacturing system controller with Petri-net enabled algebraic deadlock avoidance*, Reports in Mechanical Engineering, 1(1), pp. 77-92.